Proceedings of IMECE2002
ASME International Mechanical Engineering Congress & Exposition
November 17–22, 2002, New Orleans, Louisiana

IMECE2002-39139

SLOW PASSAGE THROUGH RESONANCE IN MATHIEU'S EQUATION

Leslie Ng
Department of Theoretical and Applied Mechanics
Cornell University
Ithaca NY 14853
Email: lhn2@cornell.edu

Richard Rand
Michael O'Neil
Department of Theoretical and Applied Mechanics
Cornell University
Ithaca NY 14853
Email: rhr2@cornell.edu

ABSTRACT

We investigate slow passage through the 2:1 resonance tongue in Mathieu's equation. Using numerical integration, we find that amplification or de-amplification can occur. The amount of amplification (or de-amplification) depends on the speed travelling through the tongue and the initial conditions. We use the method of multiple scales to obtain a slow flow approximation. The WKB method is then applied to the slow flow equations to get an analytic approximation.

INTRODUCTION

Mathieu's equation is the following second order linear non-autonomous ordinary differential equation (ODE):

$$\frac{d^2x}{dt^2} + (\delta + \varepsilon\cos t)x = 0 \tag{1}$$

Eq.(1) has be widely studied [1]. For given values of the parameters δ and ε, either all the solutions are bounded (*stable*) or an unbounded solution exists (*unstable*). Fig.1 shows the transition curves separating regions of instability from those of stability for Eq.(1) in the δ-ε parameter plane. These regions of instability are commonly referred to as resonance tongues.

In this work we investigate what happens if δ changes slowly in time. In particular, we assume δ varies linearly with time and replace δ in Eq.(1) with:

$$\delta = \sigma + \varepsilon^2\mu t \tag{2}$$

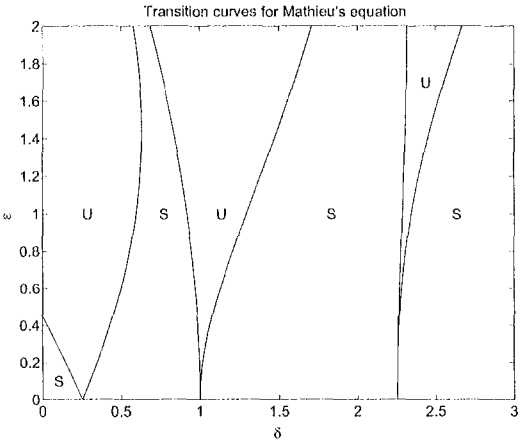

Figure 1. Regions of stability and instability in Mathieu's Equation (S=stable, U=unstable)

For fixed values of ε, we can think of a point (δ, ε) moving in time across the δ-ε plane in and out of the tongues of instability. The constant term σ is the initial value of δ at time $t = 0$ and $\varepsilon^2\mu$ is the speed at which the point (δ, ε) moves across the δ-ε plane. Putting Eq.(2) in Eq.(1) results in the following ODE:

$$\frac{d^2x}{dt^2} + (\sigma + \varepsilon^2\mu t + \varepsilon\cos t)x = 0 \tag{3}$$

which we will study using numerical integration and perturbation

methods for small values of ε.

Previous work by Nayfeh and Asfar [2] and Neal and Nayfeh [3] have investigated slow passage through resonance in Mathieu's equation with additional cubic and damping terms. After using the method of multiple scales to derive a slow flow, they perform a numerical investigation of the slow flow and report the different phenomena observed.

Raman, Bajaj and Davies [4] present a general methodology for analyzing slow passage across instabilities in non-linear dissipative systems. In [4] they present some analytic results for the system studied by Nayfeh et al. In a second paper by Raman and Bajaj [5], they present some general results for Hamiltonian oscillators. As an example, they investigate slow passage through resonance in Mathieu's equation with an additional cubic nonlinearity.

The studies mentioned above all look at variations of the Mathieu equation with a nonlinear term. The effect of the nonlinearity is to include stable nontrivial solutions in the resonance tongue as opposed to just having an unbounded solution in the case of the linear Mathieu equation. Their analysis focuses on the transition from the trivial solution to the bifurcating solution while going through the resonance tongue.

In contrast to these works, in this paper we focus on passage through resonance in the linear Mathieu equation and the question of *amplification* to be described in the next section.

NUMERICAL INTEGRATION

We begin our study by numerically integrating Eq.(3) to get an idea of what occurs when crossing a resonance tongue of Mathieu's equation. The 2:1 resonance in Mathieu's equation is the most prominant so we choose parameter values and initial conditions that would correspond to transversing the 2:1 resonance tongue from left to right in the δ-ε plane for a fixed value of ε.

For small values of ε, the first term approximation of the transition curves of the $2:1$ resonance tongue in Mathieu's equation is:

$$\delta = \frac{1}{4} \pm \frac{\varepsilon}{2} + O(\varepsilon^2), \quad \varepsilon << 1 \tag{4}$$

The minus sign corresponds to the left transition curve and the plus sign corresponds to the right transition curve. Replacing δ in Eq.(4) with Eq.(2) we have:

$$\sigma + \varepsilon^2 \mu t \approx \frac{1}{4} \pm \frac{\varepsilon}{2} \tag{5}$$

From Eq.(5), we can solve for the times that would correspond to being on the left transistion curve t_- and on the right transition curve t_+:

$$t_- \approx \frac{1 - 4\sigma}{4\varepsilon^2\mu} - \frac{1}{2\varepsilon\mu}, \quad t_+ \approx \frac{1 - 4\sigma}{4\varepsilon^2\mu} + \frac{1}{2\varepsilon\mu} \tag{6}$$

For our numerical integrations, we choose initial condition such that:

$$x(t_0) = \cos\gamma, \quad \frac{dx}{dt}(t_0) = \sin\gamma \tag{7}$$

where $0 \leq \gamma < 2\pi$.

Fig.2 shows a numerical integration for $\varepsilon = 0.1$, $\mu = 0.1$, $\sigma = 0$ and $t_0 = 0$ and $\gamma = 0$. Also shown in dashed lines are the times that would correspond to being on the transition curves ($t_- = 200$ and $t_+ = 300$).

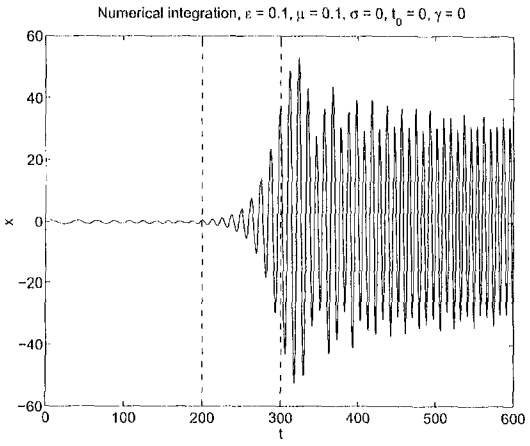

Figure 2. Numerical Integration of Eq.(3) for $\gamma = 0$, that is for $x(0) = 1$, $\frac{dx}{dt} = 0$. Note that the vertical axis is scaled to a maximum of 60. Parameters are $\varepsilon = 0.1, \mu = 0.1$ and $\sigma = 0$. Dashed vertical lines show approximate times at which the motion crosses the transition curves in the Mathieu equation (1), $t_- = 200$ and $t_+ = 300$.

Fig.3 shows a numerical integration with the same parameter values as Fig.2 but with different initial conditions ($\gamma = \pi/2$). Comparing Fig.2 and Fig.3 we see that they both exhibit amplification as a result of going through the resonance tongue although the maximum amplitude in Fig.3 is considerably larger than that

in Fig.2. Also note that in both Figs.2 and 3, the maximum amplitude occurs at the time which is larger than t_+, that is, after the motion has exited the resonance tongue.

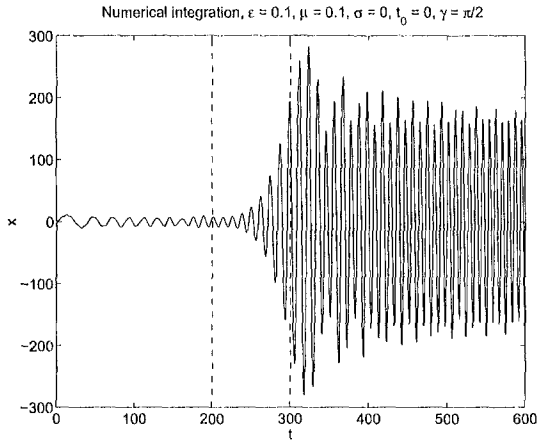

Figure 3. Numerical Integration of Eq.(3) for $\gamma = \frac{\pi}{2}$, that is for $x(0) = 0$, $\frac{dx}{dt} = 1$. Note that the vertical axis is scaled to a maximum of 300. Parameters are $\varepsilon = 0.1, \mu = 0.1$ and $\sigma = 0$. Dashed vertical lines show approximate times at which the motion crosses the transition curves in the Mathieu equation (1), $t_- = 200$ and $t_+ = 300$.

To investigate the effects of initial conditions on amplification we numerically integrate Eq.(3) for the same parameter values using a range of initial conditions ($0 \leq \gamma < 2\pi$). Fig.4 shows a plot of the maximum value of x as a function of the initial condition parameter γ. We see that the amplification can vary significantly depending on the initial conditions. Fig.5 shows a numerical integration for the initial condition $\gamma = 2.9558$ which is approximately the value of γ which has the least amplification in Fig.4. For $\gamma = 2.9558$ we see that the maximum amplitude is smaller after going through the tongue than it was prior to entering the tongue. We find that a small range of initial conditions results in deamplification after going through the resonance tongue.

SLOW-FLOW EQUATIONS

We use the method of multiple scales ([6],[7]) to obtain an analytic approximation for Eq.(3) around the 2:1 resonance tongue ($\sigma = 1/4$) for $\varepsilon << 1$. Here we set $\sigma = 1/4$ so that at $t = 0$ we are located exactly at the 2:1 resonance $\delta = 1/4$, that is, in the middle of the associated tongue of instability. We start by introducing slow and fast time variables $\eta = \varepsilon t$ and $\xi = t$. Eq.(3) becomes:

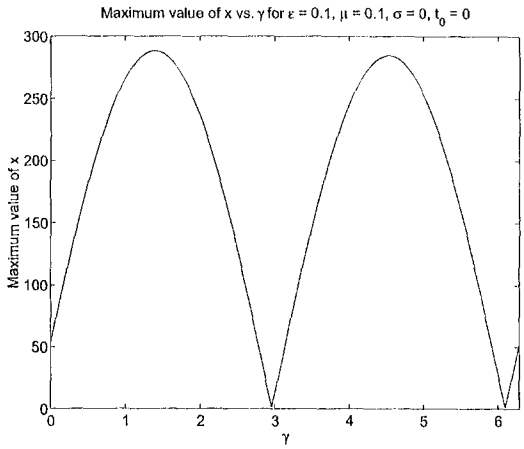

Figure 4. Maximum value of x as a function of initial condition parameter γ where γ is defined in Eq.(7). Parameters are $\varepsilon = 0.1$, $\mu = 0.1$ and $\sigma = 0$.

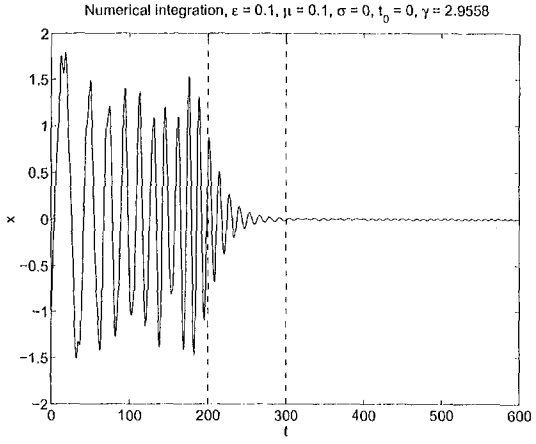

Figure 5. Numerical Integration of Eq.(3) for $\gamma = 2.9558$. Note that the vertical axis is scaled to a maximum of 2. Parameters are $\varepsilon = 0.1$, $\mu = 0.1$ and $\sigma = 0$. Dashed vertical lines show approximate times at which the motion crosses the transition curves in the Mathieu equation (1), $t_- = 200$ and $t_+ = 300$.

$$\frac{\partial^2 x}{\partial \xi^2} + 2\varepsilon \frac{\partial^2 x}{\partial \xi \partial \eta} + \varepsilon^2 \frac{\partial^2 x}{\partial^2 \eta} + (\frac{1}{4} + \varepsilon\mu\eta + \varepsilon\cos\xi)x = 0 \qquad (8)$$

Taking $x(\xi,\eta)$ as a power series $x(\xi,\eta) = x_0(\xi,\eta) + \varepsilon x_1(\xi,\eta) + \ldots$ and collecting $O(1)$ and $O(\varepsilon)$ terms gives:

$$O(1): \frac{\partial^2 x_0}{\partial \xi^2} + \frac{1}{4}x_0 = 0 \tag{9}$$

$$O(\varepsilon): \frac{\partial^2 x_1}{\partial \xi^2} + \frac{1}{4}x_1 = -2\frac{\partial^2 x_0}{\partial \xi \partial \eta} - x_0 \cos\xi - \mu\eta x_0 \tag{10}$$

The general solution of Eq.(9) is:

$$x_0(\xi,\eta) = A(\eta)\cos\frac{\xi}{2} + B(\eta)\sin\frac{\xi}{2} \tag{11}$$

Substituting Eq.(11) into Eq.(10) and simplifying trigonometric terms gives:

$$\frac{\partial^2 x_1}{\partial \xi^2} + \frac{1}{4}x_1 = \left(\frac{dA}{d\eta} - \mu\eta B\right)\sin\frac{\xi}{2} - \left(\frac{dB}{d\eta} + \mu\eta A\right)\cos\frac{\xi}{2} - \frac{A}{2}\left(\cos\frac{3\xi}{2} + \cos\frac{\xi}{2}\right) - \frac{B}{2}\left(\sin\frac{3\xi}{2} - \sin\frac{\xi}{2}\right) \tag{12}$$

Removal of secular terms results in the slow-flow equations:

$$\frac{dA}{d\eta} = (\mu\eta - \frac{1}{2})B \tag{13}$$

$$\frac{dB}{d\eta} = -(\mu\eta + \frac{1}{2})A \tag{14}$$

Eqs.(13) and (14) can be combined to form a single second order ODE in either A or B alone. Taking the derivative of Eq.(13) with respect to η gives:

$$\frac{d^2A}{d\eta^2} = (\mu\eta - \frac{1}{2})\frac{dB}{d\eta} + \mu B \tag{15}$$

Substituting Eqs.(13),(14) into Eq.(15) gives the following second order ODE in A alone:

$$\frac{d^2A}{d\eta^2} = -(\mu\eta - \frac{1}{2})(\mu\eta + \frac{1}{2})A + \frac{\mu}{\mu\eta - \frac{1}{2}}\frac{dA}{d\eta} \tag{16}$$

Setting $\tau = \mu\eta$, Eq.(16) can be rewritten as:

$$\mu^2\frac{d^2A}{d\tau^2} + (\tau^2 - \frac{1}{4})A - \frac{\mu^2}{\tau - \frac{1}{2}}\frac{dA}{d\tau} = 0 \tag{17}$$

Applying the same procedure but eliminating A gives the ODE in B:

$$\mu^2\frac{d^2B}{d\tau^2} + (\tau^2 - \frac{1}{4})B - \frac{\mu^2}{\tau + \frac{1}{2}}\frac{dB}{d\tau} = 0 \tag{18}$$

Note that Eq.(17) is singular when $\tau = 1/2$ and Eq.(18) is singular when $\tau = -1/2$.

To compare the multiple scales approximation with the original equation using numerical integration we need to relate the initial conditions of the original equation to the initial conditions of the slow flow equations. From Eq.(11), the multiple scales approximation to first order is:

$$x(t) \sim A(\eta)\cos\frac{\xi}{2} + B(\eta)\sin\frac{\xi}{2} = A(\varepsilon t)\cos\frac{t}{2} + B(\varepsilon t)\sin\frac{t}{2} \tag{19}$$

Taking the derivative with respect to time of Eq.(19) we get:

$$\frac{dx(t)}{dt} \sim \varepsilon A'(\varepsilon t)\cos\frac{t}{2} - \frac{A(\varepsilon t)}{2}\sin\frac{t}{2} + \varepsilon B'(\varepsilon t)\sin\frac{t}{2} + \frac{B(\varepsilon t)}{2}\cos\frac{t}{2} \tag{20}$$

Using Eqs.(13),(14) for $A'(\eta)$ and $B'(\eta)$, Eq.(20) can be written as:

$$\frac{dx(t)}{dt} \sim \left(\varepsilon(\mu\varepsilon t - \frac{1}{2}) + \frac{1}{2}\right)B(\varepsilon t)\cos\frac{t}{2} + \left(-\varepsilon(\mu\varepsilon t + \frac{1}{2}) - \frac{1}{2}\right)A(\varepsilon t)\sin\frac{t}{2} \tag{21}$$

At a time $t = t_0$, given $A(\eta_0)$, $B(\eta_0)$ (where $\eta_0 = \varepsilon t_0$) we can solve for the initial conditions $x(t_0)$, $\frac{dx}{dt}(t_0)$ using Eqs.(19) and (21). Fig.6 shows a comparison of the multiple scales approximation with the original equation, both obtained by numerical integration, for $\varepsilon = 0.1$, $\mu = 0.1$, $\sigma = 1/4$ with initial conditions $t_0 = -100$ and $A(\eta_0) = 1$, $B(\eta_0) = 0$. Note that the numerical integrations displayed in Figs.2,3,5 used $\sigma = 0$ and $t_0 = 0$, so that the initial time in those figures corresponds to $t_0 = -250$.

We can see in Fig.6 that the multiple scales solution is a good approximation to the original equation until about the middle of the resonance tongue ($t \approx 0$). As the approximation worsens the phase is still well approximated but the amplitude is a bit larger. At around $t \approx 150$ the phase starts to deviate as well. We also find that if we decrease the value of t_0 so the initial conditions are farther away from the tongue the entire approximation gets worse. This is because we are perturbing off the 2:1 resonance at $t = 0$. As $|t|$ increases we get farther away from the 2:1 resonance and the approximation is no longer valid.

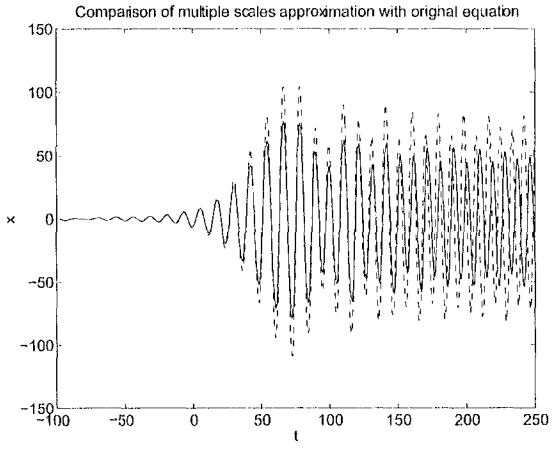

Figure 6. Comparison of multiple scales approximation with original equation. Solid line is original equation, dashed line is multiple scales approximation. Parameters are $\varepsilon = 0.1$, $\mu = 0.1$ and $\sigma = 1/4$. Initial conditions are $A(\eta_0) = 1$, $B(\eta_0) = 0$, $\eta_0 = \varepsilon t_0$, $t_0 = -100$.

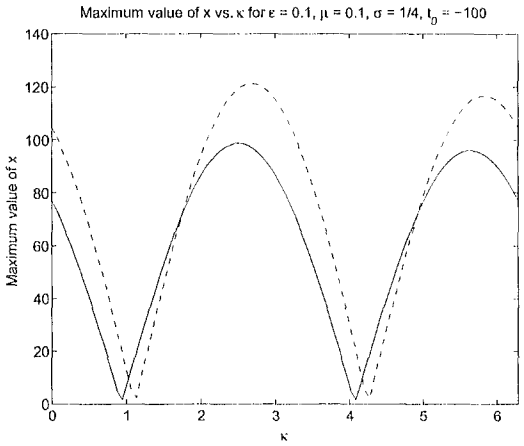

Figure 7. Comparison of multiple scales approximation with original equation. Solid line is original equation, dashed line is multiple scales approximation. Maximum Value of x as a function of initial condition parameter κ for $t_0 = -100$.

To investigate the effects of varying initial conditions, we assume the initial conditions are of the form:

$$A(\eta_0) = \cos\kappa, \quad B(\eta_0) = \sin\kappa \tag{22}$$

where $0 \leq \kappa < 2\pi$. We choose to vary initial conditions now using κ instead of γ (Eq.(7)) because it restricts $A(\eta_0)^2 + B(\eta_0)^2 = 1$. Using γ restricts $x(t_0)^2 + \frac{dx}{dt}(t_0)^2 = 1$.

As in Fig.4, we numerically integrate the original equation and the multiple scales approximation for a range of initial conditions. Fig.7 shows the maximum value of x for the multiple scales approximation and the original equation as a function of the initial condition parameter κ for $t_0 = -100$. We see that the multiple scales approximation predicts larger values but the dependence as a function of κ is still close.

Fig.8 shows a simliar plot but for $t_0 = 0$. Again, the multiple scales approximation is still larger but the dependence on κ is closer. As expected, initial conditions starting closer to $t_0 = 0$ give better approximations.

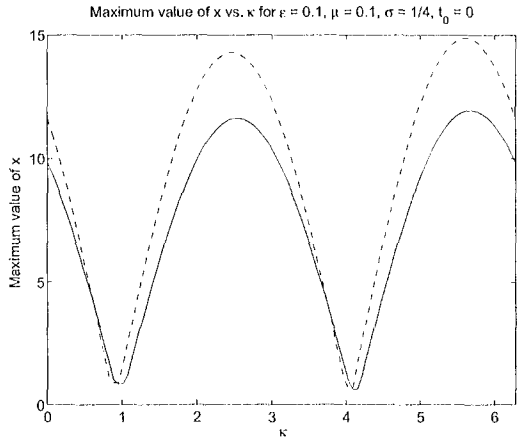

Figure 8. Comparison of multiple scales approximation with original equation. Solid line is original equation, dashed line is multiple scales approximation. Maximum Value of x as a function of initial condition parameter κ for $t_0 = 0$.

WKB APPROXIMATION

Description of the Method

The WKB method ([6],[7]) can be applied to linear ODE's where the highest derivative is multiplied by a small perturbation parameter. Eqs.(17),(18) are of the form:

$$\mu^2 y'' - q(\tau)y + \mu^2 p(\tau)y' = 0 \tag{23}$$

where the prime ($'$) denotes differentiation with respect to τ. For small values of μ, the WKB method can be applied. Application of the WKB method to Eq.(23) involves the ansatz:

$$y \sim e^{\frac{1}{\mu}\phi(\tau)}\left(y_0(\tau)+\mu y_1(\tau)+\ldots\right) \tag{24}$$

The asymptotic expansions of the first and second derivatives of the solution are:

$$y' \sim e^{\frac{1}{\mu}\phi}\left(\mu^{-1}\phi' y_0 + y_0' + \phi' y_1 + \ldots\right) \tag{25}$$

$$y'' \sim e^{\frac{1}{\mu}\phi}\left(\mu^{-2}(\phi')^2 y_0 + \mu^{-1}(\phi'' y_0 + 2\phi' y_0' + (\phi')^2 y_1) + \ldots\right) \tag{26}$$

Substituting Eqs.(25-26) into Eq.(23) gives:

$$\begin{aligned}&\mu^2\left(\mu^{-2}(\phi')^2 y_0 + \mu^{-1}(\phi'' y_0 + 2\phi' y_0' + (\phi')^2 y_1) + \ldots\right)\\ &-q(\tau)\left(y_0+\mu y_1+\ldots\right)+\mu^2 p(\tau)\left(\mu^{-1}\phi' y_0 + y_0' + \phi' y_1 + \ldots\right) = 0\end{aligned} \tag{27}$$

Collecting $O(1)$ and $O(\mu)$ terms results in the following equations:

$$O(1) : (\phi')^2 y_0 - q y_0 = 0 \tag{28}$$

$$O(\mu) : \phi'' y_0 + 2\phi' y_0' + (\phi')^2 y_1 - q y_1 + p\phi' y_0 = 0 \tag{29}$$

From Eq.(28) we have:

$$(\phi')^2 - q = 0 \Rightarrow \phi' = \pm\sqrt{q} \Rightarrow \phi = \pm\int^{\tau}\sqrt{q(s)}ds \tag{30}$$

With $\phi' = \pm\sqrt{q}$ and $\phi'' = \pm\frac{q'}{2\sqrt{q}}$, Eq.(29) becomes:

$$\pm\frac{1}{2\sqrt{q}}q' y_0 \pm 2\sqrt{q} y_0' \pm \sqrt{q} y_0 = 0 \tag{31}$$

which can be rewritten as:

$$\frac{y_0'}{y_0} = -\frac{q'}{4q} - \frac{p}{2} \tag{32}$$

Integrating Eq.(32) gives:

$$\int\frac{y_0'}{y_0} = \int\left(-\frac{q'}{4q}-\frac{p}{2}\right) \Rightarrow \log y_0 = -\frac{1}{4}\log q - \frac{1}{2}\int^{\tau} p(s)\,s \tag{33}$$

Taking the exponential of both side of Eq.(33) gives:

$$y_0(\tau) = q(\tau)^{-1/4}\, e^{-\frac{1}{2}\int^{\tau} p(s)ds} \tag{34}$$

Taking Eqs.(24),(30) and (34), the WKB approximation of Eq.(23) is:

$$y(\tau) \sim \frac{e^{-\frac{1}{2}\int^{\tau} p(s)ds}}{q(\tau)^{1/4}}\left[C_1 e^{\frac{1}{\mu}\int^{\tau}\sqrt{q(s)}ds} + C_2 e^{-\frac{1}{\mu}\int^{\tau}\sqrt{q(s)}ds}\right] \tag{35}$$

The system has a *turning point* at $\tau = \tau^*$ if $q(\tau^*) = 0$. If $q(\tau) < 0$ for $\tau < \tau^*$ and $q(\tau) > 0$ for $\tau > \tau^*$ then Eq.(35) can be written as:

$$y_L(\tau) \sim \frac{e^{-\frac{1}{2}\int^{\tau} p(s)ds}}{(-q)^{1/4}}\left[C_{L1}\cos\left(\frac{\phi_L}{\mu}+\frac{\pi}{4}\right) + C_{L2}\cos\left(\frac{\phi_L}{\mu}-\frac{\pi}{4}\right)\right],\ \tau < \tau^* \tag{36}$$

$$y_R(\tau) \sim \frac{e^{-\frac{1}{2}\int^{\tau} p(s)ds}}{q^{1/4}}\left[C_{R1}e^{\frac{\phi_R}{\mu}} + C_{R2}e^{-\frac{\phi_R}{\mu}}\right],\ \tau > \tau^* \tag{37}$$

where,

$$\phi_L = \int_{\tau}^{\tau^*}\sqrt{-q(s)}\,s, \quad \phi_R = \int_{\tau^*}^{\tau}\sqrt{q(s)}\,s$$

The approximation near the turning point depends on the form of $q(\tau)$ and $p(\tau)$. For $q'(\tau^*) \neq 0$ and $p(\tau^*) \sim const$, the solution takes the form of Airy functions. Detailed calculations will be shown for specific choices of $q(\tau)$ and $p(\tau)$. A relation between the constants C_{L1}, C_{L2} which occur in the $\tau < \tau^*$ solution (Eq.(36)) and $C_{R1} C_{R2}$ which occur in the $\tau > \tau^*$ solution (Eq.(37)) are found by matching with another approximation which is valid at the turning point.

Similarly, if $q(\tau) > 0$ for $\tau < \tau^*$ and $q(\tau) < 0$ for $\tau > \tau^*$, Eq.(35) can be written as:

$$y_L(\tau) \sim \frac{e^{-\frac{1}{2}\int^{\tau} p(s)\,s}}{q^{-1/4}}\left[C_{L1}e^{\frac{\phi_L}{\mu}} + C_{L2}e^{-\frac{\phi_L}{\mu}}\right],\ \tau < \tau^* \tag{38}$$

$$y_R(\tau) \sim \frac{e^{-\frac{1}{2}\int^{\tau} p(s)\,s}}{(-q)^{-1/4}}\left[C_{R1}\cos\left(\frac{\phi_R}{\mu}+\frac{\pi}{4}\right) + C_{R2}\cos\left(\frac{\phi_R}{\mu}-\frac{\pi}{4}\right)\right],\ \tau > \tau^* \tag{39}$$

where,

$$\phi_L = \int_{\tau}^{\tau^*}\sqrt{q(s)}ds, \quad \phi_R = \int_{\tau^*}^{\tau}\sqrt{-q(s)}\,s$$

Application to the Slow Flow

We apply the WKB method to the equation on A (Eq.(17)) obtained from the slow flow equations. In Eq.(17), $q = 1/4 - \tau^2$ so we have turning points at $\tau = \pm 1/2$. Because we have two turning points, the approximation can be divided into 5 different regions:

Table 1. Labels for Different Regions of Approximations for A

Label	Region of τ	
A_1	$\tau < -1/2$	before turning points
A_2	$\tau \approx -1/2$	near turning point at $\tau = -1/2$
A_3	$-1/2 < \tau < 1/2$	between the two turning points
A_4	$\tau \approx 1/2$	near turning point at $\tau = 1/2$
A_5	$\tau > 1/2$	after turning points

Also in Eq.(17) we have $p = \dfrac{-1}{\tau - 1/2}$ so solving for the exponential in the y_0 term in Eq.(34) gives:

$$e^{-\frac{1}{2}\int^{\tau} p(s)ds} = e^{\frac{1}{2}\int^{\tau} \frac{1}{s-1/2}ds} = e^{\frac{1}{2}\log|\tau - 1/2|} = \sqrt{|\tau - \frac{1}{2}|} \quad (40)$$

We begin by finding A_1, an expression for A valid for $\tau < -1/2$, and A_3, an expression for A valid for $-1/2 < \tau < 1/2$. For $\tau < -1/2$, $q(\tau) > 0$ and for $-1/2 < \tau < 1/2$, $q(\tau) < 0$ so the approximation is of the form of Eqs.(36),(37). Thus, the WKB approximations for A_1 and A_3 are:

$$A_1 = \frac{\left(\frac{1}{2} - \tau\right)^{1/2}}{\left(\tau^2 - \frac{1}{4}\right)^{1/4}}\left[C_{11}\cos\left(\frac{\phi_1}{\mu} + \frac{\pi}{4}\right) + C_{12}\cos\left(\frac{\phi_1}{\mu} - \frac{\pi}{4}\right)\right], \tau < -\frac{1}{2} \quad (41)$$

$$A_3 = \frac{\left(\frac{1}{2} - \tau\right)^{1/2}}{\left(\frac{1}{4} - \tau^2\right)^{1/4}}\left(C_{31}\, e^{\frac{i}{\mu}\phi_3} + C_{32}\, e^{-\frac{i}{\mu}\phi_3}\right), \ -\frac{1}{2} < \tau < \frac{1}{2} \quad (42)$$

where,

$$\phi_1 = \int_{\tau}^{-1/2} \sqrt{s^2 - \frac{1}{4}}ds = -\frac{2\tau\sqrt{4\tau^2 - 1} - \log\left(-\sqrt{4\tau^2 - 1} - 2\tau\right)}{8}$$

$$\phi_3 = \int_{-1/2}^{\tau} \sqrt{\frac{1}{4} - s^2}ds = \frac{\arcsin(2\tau) + 2\tau\sqrt{1 - 4\tau^2}}{8} + \frac{\pi}{16}$$

To obtain an approximation near the turning point at $\tau = -1/2$, we make the change of variables $z = \dfrac{\tau + 1/2}{\mu^{\beta}}$. Near the turning point, Eq.(17) behaves like:

$$\mu^{2-2\beta}A'' - z\mu A - \mu^{2-\beta}A' = 0 \quad (43)$$

Choosing $\beta = 2/3$ balances the A'' and A terms which gives the equation:

$$A'' - zA = 0 \quad (44)$$

which is just Airy's equation. The solution can be written in terms of Airy functions:

$$A_2 = C_{21}Ai(z) + C_{22}Bi(z) = C_{21}Ai\left(\frac{\tau + \frac{1}{2}}{\mu^{2/3}}\right) + C_{22}Bi\left(\frac{\tau + \frac{1}{2}}{\mu^{2/3}}\right) \quad (45)$$

Eqs.(41),(42),(45) now form the WKB approximation. The six constants (C's) can be reduced to two by matching the the solutions. To match the solutions we use asymptotic expansions of the approximations. See Appendix A for details of the matching procedure. We find the following equations relating $C_{21}, C_{22}, C_{31}, C_{32}$ to C_{11}, C_{12}:

$$C_{31} = C_{11}, \ C_{32} = \frac{C_{12}}{2}, \ C_{21} = \sqrt{\pi}\mu^{-1/4}\, C_{12}, \ C_{22} = \sqrt{\pi}\mu^{-1/6}C_1 \quad (46)$$

Our WKB approximation of A using Eq.(17) is:

$$A_1 = \frac{\left(\frac{1}{2} - \tau\right)^{1/2}}{\left(\tau^2 - \frac{1}{4}\right)^{1/4}}\left[C_{11}\cos\left(\frac{\phi_1}{\mu} + \frac{\pi}{4}\right) + C_{12}\cos\left(\frac{\phi_1}{\mu} - \frac{\pi}{4}\right)\right], \tau < -\frac{1}{2} \quad (47)$$

$$A_2 = \frac{\sqrt{\pi}}{\mu^{1/6}}\left[C_{12}Ai\left(\frac{\tau + \frac{1}{2}}{\mu^{2/3}}\right) + C_{11}Bi\left(\frac{\tau + \frac{1}{2}}{\mu^{2/3}}\right)\right], \tau \approx -\frac{1}{2} \quad (48)$$

$$A_3 = \frac{\left(\frac{1}{2} - \tau\right)^{1/2}}{\left(\frac{1}{4} - \tau^2\right)^{1/4}}\left(C_{11}\, e^{\frac{i}{\mu}\phi_3} + \frac{C_{12}}{2}\, e^{-\frac{i}{\mu}\phi_3}\right), \ -\frac{1}{2} < \tau < \frac{1}{2} \quad (49)$$

where,

$$\phi_1 = -\frac{2\tau\sqrt{4\tau^2 - 1} - \log\left(-\sqrt{4\tau^2 - 1} - 2\tau\right)}{8}$$

$$\phi_3 = \frac{\arcsin(2\tau) + 2\tau\sqrt{1 - 4\tau^2}}{8} + \frac{\pi}{16}$$

So far we have used the WKB method on the A equation (Eq.(17)). Since Eq.(17) is *singular* at $\tau = 1/2$, we now switch to the B equation (Eq.(18)) to study the behavior in the neighborhood of $\tau = 1/2$. In a similar fashion to the preceeding, we obtain:

$$B_3 = \frac{\left(\tau+\frac{1}{2}\right)^{1/2}}{\left(\frac{1}{4}-\tau^2\right)^{1/4}}\left(D_{31}\, e^{\frac{1}{\mu}\phi_3^*} + D_{32}\, e^{-\frac{1}{\mu}\phi_3^*}\right),\ -\frac{1}{2} < \tau < \frac{1}{2} \tag{50}$$

$$B_4 = \frac{\sqrt{\pi}}{\mu^{1/6}}\left[2D_{32}Ai\left(\frac{\frac{1}{2}-\tau}{\mu^{2/3}}\right) + D_{31}Bi\left(\frac{\frac{1}{2}-\tau}{\mu^{2/3}}\right)\right],\ \tau \approx \frac{1}{2} \tag{51}$$

$$B_5 = \frac{\left(\tau+\frac{1}{2}\right)^{1/2}}{\left(\tau^2-\frac{1}{4}\right)^{1/4}}\left[D_{31}\cos\left(\frac{\phi_5}{\mu}+\frac{\pi}{4}\right) + 2D_{32}\cos\left(\frac{\phi_5}{\mu}-\frac{\pi}{4}\right)\right],\ \tau > \frac{1}{2} \tag{52}$$

where,

$$\phi_3^* = \frac{\pi}{16} - \frac{\arcsin(2\tau) + 2\tau\sqrt{1-4\tau^2}}{8} = -\phi_3 + \frac{\pi}{8}$$
$$\phi_5 = \frac{2\tau\sqrt{4\tau^2-1} - \log\left(\sqrt{4\tau^2-1}+2\tau\right)}{8}$$

The approximation for B can then be used to give an approximation for A around $\tau = 1/2$ by taking the derivative of Eqs.(50-52) and using Eq.(14) which relates A to $dB/d\eta$ (or $dB/d\tau$). This avoids analyzing Eq.(17) around $\tau = 1/2$ where it is singular. Doing this we get:

$$A_3^* = -\frac{D_{31}(2\mu-(1-4\tau^2)^{3/2})e^{\frac{1}{\mu}\phi_3^*} + D_{32}(2\mu+(1-4\tau^2)^{3/2})e^{-\frac{1}{\mu}\phi_3^*}}{\sqrt{2\tau+1}(1-4\tau^2)^{5/4}} \tag{53}$$

$$A_4 = \frac{2\mu^{1/3}\sqrt{\pi}}{2\tau+1}\left[2D_{32}Ai'\left(\frac{\frac{1}{2}-\tau}{\mu^{2/3}}\right) + D_{31}Bi'\left(\frac{\frac{1}{2}-\tau}{\mu^{2/3}}\right)\right] \tag{54}$$

$$A_5 = \left[\left(2D_{31}\mu - 2D_{32}(4\tau^2-1)^{3/2}\right)\cos\left(\frac{\phi_5}{\mu}+\frac{\pi}{4}\right) + \left(4D_{32}\mu + D_{31}(4\tau^2-1)^{3/2}\right)\cos\left(\frac{\phi_5}{\mu}-\frac{\pi}{4}\right)\right] / \left[\sqrt{2\tau+1}(4\tau^2-1)^{5/4}\right] \tag{55}$$

where,

$$\phi_3^* = \frac{\pi}{16} - \frac{\arcsin 2\tau + 2\tau\sqrt{1-4\tau^2}}{8}$$
$$\phi_5 = \frac{2\tau\sqrt{4\tau^2-1} - \log(\sqrt{4\tau^2-1}+2\tau)}{8}$$

We have two approximations for A in the region between the two turning points: A_3 (from applying the WKB method on Eq.(17)) and A_3^* (from applying the WKB method on Eq.(18) and then using Eq.(14)). To combine the two approximations we take A_3 for $\tau \le 0$ and A_3^* for $\tau \ge 0$ and match A_3 to A_3^* and their derivatives at $\tau = 0$ requiring:

$$A_3(0) = A_3^*(0) \quad \text{and} \quad \frac{dA_3}{d\tau}(0) = \frac{dA_3^*}{d\tau}(0) \tag{56}$$

Doing this we obtain the following relations between D_{31}, D_{32} and C_{11}, C_{12}:

$$D_{31} = -\frac{C_{12}}{2(2\mu-1)}e^{-\frac{\pi}{8\mu}} \tag{57}$$

$$D_{32} = -\frac{C_{11}}{2\mu+1}e^{\frac{\pi}{8\mu}} \tag{58}$$

Finally we must be able to solve for C_{11},C_{12} in terms of the initial conditions $A(\tau_0)$, $B(\tau_0)$. Let us assume that our initial conditions are prescribed for $\tau_0 < -1/2$ (i.e. before the motion enters the resonance tongue) so $A(\tau_0) = A_1(\tau_0)$. We can obtain $B(\tau_0)$ from $A_1(\tau_0)$ using Eq.(13). The equations relating $A(\tau_0)$, $B(\tau_0)$ to C_{11}, C_{12} are:

$$A(\tau_0) = \quad A_1(\tau_0) \quad = K_{11}(\tau_0)C_{11} + K_{12}(\tau_0)C_{12} \tag{59}$$

$$B(\tau_0) = \frac{\mu}{\tau_0 - \frac{1}{2}}\frac{dA_1}{d\tau}(\tau_0) = K_{21}(\tau_0)C_{11} + K_{22}(\tau_0)C_{12} \tag{60}$$

See Appendix B for the expressions for $K_{ij}(\tau_0)$. Eqs.(59),(60) can be expressed in matrix form:

$$\begin{bmatrix} A(\tau_0) \\ B(\tau_0) \end{bmatrix} = \begin{bmatrix} K_{11}(\tau_0) & K_{12}(\tau_0) \\ K_{21}(\tau_0) & K_{22}(\tau_0) \end{bmatrix}\begin{bmatrix} C_{11} \\ C_{12} \end{bmatrix} \tag{61}$$

We can find C_{11}, C_{12} in terms of $A(\tau_0)$, $B(\tau_0)$ using the inverse of the $K_{ij}(\tau_0)$ matrix:

$$\begin{bmatrix} C_{11} \\ C_{12} \end{bmatrix} = \begin{bmatrix} K_{11}(\tau_0) & K_{12}(\tau_0) \\ K_{21}(\tau_0) & K_{22}(\tau_0) \end{bmatrix}^{-1}\begin{bmatrix} A(\tau_0) \\ B(\tau_0) \end{bmatrix} \tag{62}$$

Finally, our WKB approximation of A is given by Eqs.(47-49),(53-55) and (57-58). The constants C_{11}, C_{12} are related to the initial conditions $A(\tau_0)$,$B(\tau_0)$ by Eq.(62). An expression for B can be obtained using the A approximation and Eq.(13).

Fig.9 shows a comparison of the WKB approximation with numerical integration of the slow flow equations for $\mu = 0.1$, $\tau_0 = -2.5$ and the initial conditions $A(\tau_0) = 1, B(\tau_0) = 0$. Fig.10 shows a close up of Fig.9 for the region around the first turning point. The approximation is nearly indistinguishable from the numerical integration prior to the second turning point. Around the second turning point, the error becomes more significant and the amplitude is smaller in the approximation. However, the phase is well approximated throughout the solution.

Recall that the multiple scales approximation gets worse as we get farther away from the 2:1 resonance ($|t|$ gets larger), see Fig.6. Because the WKB approximation is based on the slow flow equations, it too is only good for values of $|t|$ (or $|\eta|$ and $|\tau|$) that are not too large.

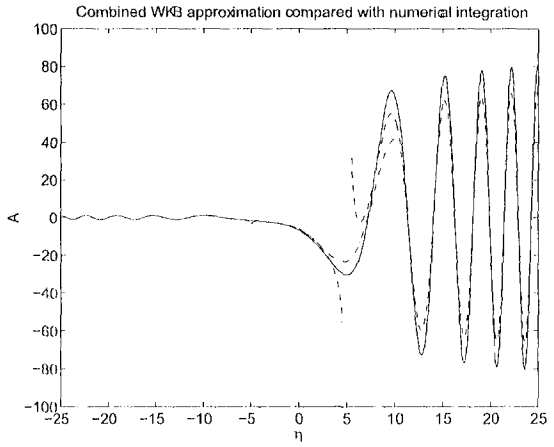

Figure 9. Comparison of WKB approximation with numerical integration of slow flow. Solid line is numerical integration, dashed lines are WKB approximations away from turning points (A_1,A_3,A_3^*,A_5) and dashed-dotted lines are WKB approximations at turning points (A_2,A_4). Parameters are $\mu = 0.1$, $\tau_0 = -2.5$, $\eta_0 = -25$ amd initial conditions are $A(\tau_0) = 1$, $B(\tau_0) = 0$.

AMPLIFICATION IN RESONANCE REGION

The WKB analysis performed can help us understand the phenomena of amplification (or deamplification) in the resonance region. The turning points in our WKB analysis correspond to the transition curves of the resonance region. At the turning points, the nature of the solution changes from oscillatory to exponential. Outside the resonance region, the WKB approximation has oscillatory solutions so amplification does not occur. Inside the resonance region, the WKB approximation has

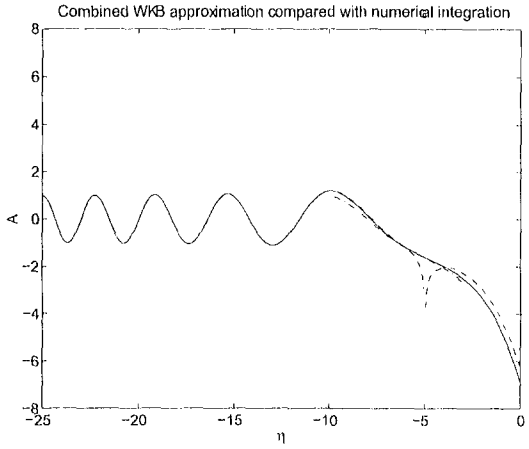

Figure 10. Comparison of WKB approximation with numerical integration of slow flow. This figure is an enlargement of Fig.9. Solid line is numerical integration, dashed lines are WKB approximation away from turning points (A_1,A_3) and dashed-dotted line is WKB approximation at turning point (A_2). Parameters are $\mu = 0.1$, $\tau_0 = -2.5$, $\eta_0 = -25$ amd initial conditions are $A(\tau_0) = 1$, $B(\tau_0) = 0$.

exponentially growing and decaying solutions which can result in amplification (or deamplification).

The WKB approximation can be used to determine which initial conditions result in the smallest oscillation amplitude after passing through the resonance tongue. The initial conditions should be chosen so that the WKB approximation between the turning points (A_3), that is, inside the resonant tongue, does not have an exponentially growing component. This requires the constant $C_{11} = 0$ (see Eq.(49)). The initial conditions leading to maximum deamplification can be found using Eq.(61):

$$\begin{bmatrix} A(\tau_0) \\ B(\tau_0) \end{bmatrix} = \begin{bmatrix} K_{11}(\tau_0) & K_{12}(\tau_0) \\ K_{21}(\tau_0) & K_{22}(\tau_0) \end{bmatrix} \begin{bmatrix} 0 \\ C_{12} \end{bmatrix} \tag{63}$$

which gives:

$$A(\tau_0) = K_{12}(\tau_0)C_{12}, \quad B(\tau_0) = K_{22}(\tau_0)C_{12} \tag{64}$$

If we again assume initial conditions of the form of Eqs.(22), we can solve for the value of κ which gives the maximum deamplification:

$$\tan\kappa_{min} = \frac{B(\tau_0)}{A(\tau_0)} = \frac{K_{22}(\tau_0)}{K_{12}(\tau_0)} \Rightarrow \kappa_{min} = \arctan\left(\frac{K_{22}(\tau_0)}{K_{12}(\tau_0)}\right) \tag{65}$$

Using the expressions for $K_{12}(\tau_0)$ and $K_{22}(\tau_0)$ in Appendix B, we obtain:

$$\kappa_{min} = \arctan\left(\frac{(4\tau_0^2-1)^{3/2}\cos\left(\frac{\phi_1(\tau_0)}{\mu}+\frac{\pi}{4}\right)-2\mu\cos\left(\frac{\phi_1(\tau_0)}{\mu}-\frac{\pi}{4}\right)}{(1-2\tau_0)(4\tau_0^2-1)^{3/2}\sin\left(\frac{\phi_1(\tau_0)}{\mu}-\frac{\pi}{4}\right)}\right) \quad (66)$$

where $\phi_1(\tau_0)$ is given by Eq.(78) in Appendix B.

We can also obtain an expression for κ_{max} where the maximum amplification occurs by taking $C_{12} = 0$ instead of C_{11} and repeating the calculation above.

For $\mu = 0.1$, $\tau_0 = -1$, using Eq.(66) we get $\kappa_{min} = 1.0328$. Numerical integration of the slow flow equations shows maximum deamplification occurs when $\kappa \approx 1.1123$ which is close to the value predicted by the WKB method. For $\varepsilon = 0.1$, numerical integration of the original equation, for this case in which $\mu = 0.1$, $\tau_0 = -1$, $t_0 = -100$, shows maximum deamplification occurs when $\kappa \approx 0.9304$ which is again close to the value predicted by the WKB method (see Fig.7).

CONCLUSIONS

We have found that amplification/deamplification can occur for slow passage through resonance in Mathieu's equation. The degree of amplification depends on the initial conditions. A very small range of initial conditions can lead to deamplification.

Using the method of multiple scales we have obtained a system of slow flow equations which approximates Eq.(3) around the 2:1 resonance. The WKB method was applied to the slow flow equations. Turning points in the WKB approximation correspond to the transition curves of the linear Mathieu equation. Outside of the resonance tongue, the WKB approximation has oscillatory solutions and inside the tongue the WKB approximation has exponentially growing and decaying solutions. By choosing the constants of the WKB approximation such that there is only a decaying solution in the resonance region we can obtain an approximation for the initial conditions in the slow flow which result in the smallest amplitude after passing through the tongue.

ACKNOWLEDGEMENTS

This work was partially supported by the Natural Sciences and Engineering Research Council of Canada (NSERC), the Office of Naval Research, Program Officer Dr. Roy Elswick, Code 321 and the National Space Grant College and Fellowship Program, NASA/NY Space Grant Consortium under Grant No. NGT5-40078.

REFERENCES

[1] Stoker, J. J., *Nonlinear Vibrations in Mechanical and Electrical Systems*, Wiley, New York, 1950.

[2] Nayfeh, A. H., Asfar, K. R., "Non-stationary Parametric Oscillations" *Journal of Sound and Vibration*, 124(3), 1988, pp. 529-537.

[3] Neal, H. L., Nayfeh, A. H., "Response of a Single-Degree-of-Freedom System to a Non-Stationary Principal Parametric Excitation" *International Journal of Non-Linear Mechanics*, Vol.25, No.2/3, 1990, pp. 275-284.

[4] Raman, A., Bajaj, A. K., Davies, P., "On the Slow Transition Across Instabilities in Non-Linear Dissipative Systems" *Journal of Sound and Vibration*, 192(4), 1996, pp. 835-865.

[5] Raman, A., Bajaj, A. K., "On the Non-Stationary Passage Through Bifurcations in Resonantly Forced Hamiltonian Oscillators" *International Journal of Non-Linear Mechanics*, Vol.33, No.5, 1998, pp. 907-933.

[6] Holmes, M. H., *Introduction to Perturbation Methods*, Springer-Verlag, New York, 1995.

[7] Bender, C. M., Orszag, S. A., *Advanced Mathematical Methods for Scientists and Engineers*, Springer-Verlag, New York, 1999.

Appendix A

Matching different parts of the WKB approximation requires using their asymptotic expansions. The asymptotic expansions of Eq.(48) are:

$$A_2 \sim \frac{z^{1/4}}{2\sqrt{\pi}}\left[C_{21}e^{-\frac{2}{3}z^{3/2}} + 2C_{22}e^{\frac{2}{3}z^{3/2}}\right],\ z \to \infty \quad (67)$$

$$A_2 \sim \frac{|z|^{1/4}}{\sqrt{\pi}}\left[C_{21}\cos\left(\frac{2}{3}|z|^{3/2}-\frac{\pi}{4}\right)+C_{22}\cos\left(\frac{2}{3}|z|^{3/2}+\frac{\pi}{4}\right)\right],\ z \to -\infty \quad (68)$$

where $z = \dfrac{\tau+\frac{1}{2}}{\mu^{2/3}}$

The asymptotic expansions of Eqs.(47),(49) are:

$$A_1 \sim \frac{|z|^{-1/4}}{\mu^{1/6}}\left(C_{11}\cos(\frac{2}{3}|z|^{3/2}+\frac{\pi}{4})+C_{12}\cos(\frac{2}{3}|z|^{3/2}-\frac{\pi}{4})\right),\ \tau \to -\frac{1}{2} \quad (69)$$

$$A_3 \sim \frac{z^{-1/4}}{\mu^{1/6}}\left(C_{31}e^{\frac{2}{3}z^{3/2}} + C_{32}e^{-\frac{2}{3}z^{3/2}}\right),\ \tau \to -\frac{1}{2} \quad (70)$$

Equating the coefficients in Eq.(67) to Eq.(70) and Eq.(68) to Eq.(69) gives the following equations relating $C_{21}, C_{22}, C_{31}, C_{32}$ to C_{11}, C_{12}:

$$C_{21} = \sqrt{\pi}\mu^{-1/6}\,C_{12},\ C_{22} = \sqrt{\pi}\mu^{-1/6}\,C_{11},\ C_{31} = C_{11},\ C_{32} = \frac{C_{12}}{2} \quad (71)$$

The asymptotic expansions of Eq.(51) are:

$$B_4 \sim \frac{z^{-1/4}}{\sqrt{\pi}}\Big[D_{41}\cos\Big(\frac{2}{3}z^{3/2}-\frac{\pi}{4}\Big)+D_{42}\cos\Big(\frac{2}{3}z^{3/2}+\frac{\pi}{4}\Big)\Big],\ z\to\infty \tag{72}$$

$$B_4 \sim \frac{|z|^{-1/4}}{2\sqrt{\pi}}\Big[D_{41}e^{-\frac{2}{3}|z|^{3/2}}+2D_{42}e^{\frac{2}{3}|z|^{3/2}}\Big],\ z\to-\infty \tag{73}$$

where $z=\dfrac{\tau-\frac{1}{2}}{\mu^{2/3}}$.

The asymptotic expansions of Eqs.(50),(52) are:

$$B_3 \sim \frac{|z|^{-1/4}}{\mu^{1/6}}\Big[D_{31}e^{\frac{2}{3}|z|^{3/2}}+D_{32}e^{-\frac{2}{3}|z|^{3/2}}\Big],\ \tau\to\frac{1}{2} \tag{74}$$

$$B_5 \sim \frac{z^{-1/4}}{\mu^{1/6}}\Big[D_{51}\cos\Big(\frac{2}{3}z^{3/2}+\frac{\pi}{4}\Big)+D_{52}\cos\Big(\frac{2}{3}z^{3/2}-\frac{\pi}{4}\Big)\Big],\ \tau\to\frac{1}{2} \tag{75}$$

Equating the coefficients in Eq.(72) to Eq.(75) and Eq.(73) to Eq.(74) gives the following equations relating D_{41}, D_{42}, D_{51}, D_{52} to D_{31}, D_{32}:

$$D_{41}=2\sqrt{\pi}\mu^{-1/6}D_{32},\ D_{42}=\sqrt{\pi}\mu^{-1/6}D_{31},\ D_{51}=D_{31},\ D_{52}=2D_{32} \tag{76}$$

Appendix B

Expressions are given for $K_{ij}(\tau_0)$ which relate initial conditions of the slow flow equations ($A(\tau_0)$, $B(\tau_0)$) to the constants in the WKB aproximation (C_{11}, C_{12}). From Eq.(59) we have:

$$\begin{aligned}A(\tau_0) &= A_1(\tau_0)=K_{11}(\tau_0)C_{11}+K_{12}(\tau_0)C_{12}\\ &= \frac{\left(\frac{1}{2}-\tau_0\right)^{1/2}}{\left(\tau_0^2-\frac{1}{4}\right)^{1/4}}\Big[C_{11}\cos\Big(\frac{\phi_1(\tau_0)}{\mu}+\frac{\pi}{4}\Big)+C_{12}\cos\Big(\frac{\phi_1(\tau_0)}{\mu}-\frac{\pi}{4}\Big)\Big]\end{aligned} \tag{77}$$

where,

$$\phi_1(\tau_0) = -\frac{2\tau_0\sqrt{4\tau_0^2-1}-\log\Big(-\sqrt{4\tau_0^2-1}-2\tau_0\Big)}{8} \tag{78}$$

Collecting terms in Eq.(77), we get:

$$K_{11}(\tau_0)=\frac{\left(\frac{1}{2}-\tau_0\right)^{1/2}}{\left(\tau_0^2-\frac{1}{4}\right)^{1/4}}\cos\Big(\frac{\phi_1(\tau_0)}{\mu}+\frac{\pi}{4}\Big) \tag{79}$$

$$K_{12}(\tau_0)=\frac{\left(\frac{1}{2}-\tau_0\right)^{1/2}}{\left(\tau_0^2-\frac{1}{4}\right)^{1/4}}\cos\Big(\frac{\phi_1(\tau_0)}{\mu}-\frac{\pi}{4}\Big) \tag{80}$$

From Eq.(60) we have:

$$\begin{aligned}B(\tau_0) &= \frac{\mu}{\tau_0-\frac{1}{2}}\frac{dA_1}{d\tau}(\tau_0)=K_{21}(\tau_0)C_{11}+K_{22}(\tau_0)C_{12}\\ &= -\Big[\Big(2C_{11}\mu-C_{12}(4\tau_0^2-1)^{3/2}\Big)\cos\Big(\frac{\phi_1(\tau_0)}{\mu}+\frac{\pi}{4}\Big)\\ &\quad+\Big(2C_{12}\mu+C_{11}(4\tau_0^2-1)^{3/2}\Big)\cos\Big(\frac{\phi_1(\tau_0)}{\mu}-\frac{\pi}{4}\Big)\Big]/\\ &\quad\Big[\sqrt{1-2\tau_0}(4\tau_0^2-1)^{5/4}\Big]\end{aligned} \tag{81}$$

Collecting terms in Eq.(81), we get:

$$K_{21}(\tau_0) = -\Big[\,2\mu\cos\Big(\frac{\phi_1(\tau_0)}{\mu}+\frac{\pi}{4}\Big)+(4\tau_0^2-1)^{3/2}\cos\Big(\frac{\phi_1(\tau_0)}{\mu}-\frac{\pi}{4}\Big)\,\Big]/\Big[\sqrt{1-2\tau_0}(4\tau_0^2-1)^{5/4}\Big] \tag{82}$$

$$K_{22}(\tau_0) = \Big[\,(4\tau_0^2-1)^{3/2}\cos\Big(\frac{\phi_1(\tau_0)}{\mu}+\frac{\pi}{4}\Big)-2\mu\cos\Big(\frac{\phi_1(\tau_0)}{\mu}-\frac{\pi}{4}\Big)\Big]/\Big[\sqrt{1-2\tau_0}(4\tau_0^2-1)^{5/4}\Big] \tag{83}$$